Journal of Hazardous Materials 172 (2009) 1137–1144

Contents lists available at ScienceDirect

Journal of Hazardous Materials

journal homepage: www.elsevier.com/locate/jhazmat

Removal of copper from aqueous solution using iron-containing adsorbents derived from methane fermentation sludge

Qingrong Qian*, Kazuhiro Mochidzuki, Takao Fujii, Akiyoshi Sakoda

Institute of Industrial Science, The University of Tokyo, 4-6-1 Komaba, Meguro-ku, Tokyo 153-8505, Japan

ARTICLE INFO

Article history:
Received 20 May 2009
Received in revised form 24 July 2009
Accepted 24 July 2009
Available online 3 August 2009

Keywords:
Copper
Adsorption
Iron-enriched adsorbent
Methane fermentation sludge
Adsorption mechanism

ABSTRACT

Iron-containing adsorbents prepared from methane fermentation sludge (MFS) were characterized by N_2 adsorption, XRD, SEM, EDX, pH determination and elemental analysis. The experiments for copper removal from aqueous solution using the MFS-derived adsorbents were performed, and the effects of iron content, forms of the iron (hydr)oxides, surface basicity and pH of the aqueous solution on copper removal were elucidated respectively. The desorption studies were also performed and the mechanism of Cu(II) adsorption was proposed. The results indicated that the adsorbent obtained at 700 °C for 1 h in a steam atmosphere possessed the highest capability for Cu(II) adsorption. The high copper removal ability of the MFS-derived materials is attributed to their intermediate surface area, strong surface basicity and the presence of iron (hydr)oxides on their surface. The Cu(II) adsorption onto the composite adsorbents is via ion-exchange with H, Ca and K ions, surface precipitation and binding with active sites on the surface of iron (hydr)oxides at various pH values. The desorption of copper in deionized water is quite low. The irreversibility of copper adsorption on the iron-containing adsorbents is attributed to the formation of strong bonds between Cu(II) and the iron (hydr)oxides. The adsorbent can be applied to remove copper from water or soil by fixation onto the surface.

1. Introduction

The amount of domestic animal excreta generated in Japan reaches 100 million tons per year. Methane fermentation has been extensively employed to treat this waste due to its merits of pollution control and energy recovery. However, the disposal of methane fermentation sludge (MFS) which is a residue separated by coagulation from digestion liquid after the anaerobic process is still difficult and expensive because of its complex composition. It has been recognized that the efficient method of sludge recycling and minimization is via pyrolysis. The pyrolysis conditions can be adjusted toward obtaining the most effective adsorbents for a desired application [1–3]. The produced adsorbents can be used for removing dyes [4–6], heavy metals [7–9], phenols [10], chloroform [11] and other organic materials [12] or hydrogen sulfide [13,14]. Their high removal capacity is a result of complexity of surface chemistry, specific porosity, and high volume of mesopores.

On the other hand, heavy metal ions have become an ecotoxicological hazard of prime interest and increasing significance because of their accumulation in living organisms. One of these metals is copper, which has been reported to cause liver toxicity, jaundice, neurotoxicity and linked with an increase in lung cancer among exposed workers [15]. Removal of these heavy metals from water is now an important environmental problem. It is well known and established that metal oxides such as iron oxides or hydroxides can adsorb toxic metals [16,17] and other trace elements [18] onto their surface or can incorporate them into their structure. Compared with activated carbons, metal oxides or hydroxides have higher metals affinities and adsorption. The strong bonding of heavy metal ions to the surface of metal oxides or hydroxides is due to the formation of inner-sphere metal surface complexes and metal hydroxide precipitate phases [19,20]. Furthermore, metal (hydr)oxides have the ability to remove and lower metals to trace concentrations. However, solid separation and management after the adsorption process can be difficult, because the metal (hydr)oxides are usually in colloidal forms [21]. Recently many efforts have been focused on composite materials to solve this problem. Composite adsorbents of this type, including FeOOH-coated maghemite [22], TiO_2-supported iron oxide [23] and iron-modified GAC [24], have been synthesized for the removal of heavy metals. Results from the above studies suggested that the composite adsorbents can be easily separated from aqueous solution after the adsorption process.

In this study, methane fermentation sludge was employed as a precursor to prepare iron-containing adsorbents. The surface features were characterized using N_2 adsorption, elemental analysis, SEM, XRD, EDX and pH determination. The performance of the pre-

* Corresponding author. Tel.: +81 043 251 4327; fax: +81 043 251 1231.
E-mail address: qrqian@iis.u-tokyo.ac.jp (Q. Qian).

0304-3894/$ – see front matter © 2009 Elsevier B.V. All rights reserved.
doi:10.1016/j.jhazmat.2009.07.107

pared adsorbents in the process of copper removal from aqueous solution was investigated. The desorption of Cu(II) was also performed to evaluate the irreversibility of Cu(II) adsorption on the adsorbents. The mechanism of Cu(II) adsorption was proposed.

2. Experimental

2.1. Preparation of adsorbents

The methane fermentation sludge used in this study was supplied from a biogas plant (a demonstration facility in which the bio-recycle project for methane fermentation of cattle excreta has been performed). The residue was coagulated and separated from the digestion liquid after the anaerobic process by using a mixed coagulator containing an organic polymer (LEC-111, Ebara Engineering Service Corp., Japan) and a polyferric sulphate $[Fe_2(OH)_n(SO_4)_{3-n/2}]$ (Nittetsu Mining Corp., Japan). The as-received MFS contained 79.6% moisture. After being dried in an oven at 105 °C overnight, the MFS was ground and sieved into a size range of 0.5–1.7 mm (30–10 mesh). The compositions of dry basis of MFS were determined and are listed in Table 1. The variation in composition of MFS from various locations was below 2.0%. Carbonization experiment was carried out in a quartz tube using a horizontal tubular furnace. 10 g of dried MFS on a ceramic boat was placed inside the quartz tube and pyrolyzed at 500 °C for 1 h in nitrogen atmosphere. The heating rate was 10 °C/min and the nitrogen flow rate was 200 mL/min. The preparing conditions of MFS-derived materials are shown in Table 1. All samples were rinsed with hot deionized water to a constant pH value and subsequently dried overnight in an oven at 105 °C prior to the characterization and adsorption experiments. Two samples denoted as CF21N7 and CF21S7 were prepared from $FeNO_3$-imperganted MFS with a mass ratio of 2/1 for the sake of comparison.

2.2. Analytical methods

The N_2 adsorption–desorption isotherms of the prepared materials were measured by a surface area analyzer (BELSORP-mini, BEL Japan Inc.) at 77 K. Samples were dried at 105 °C for 1 h, and then out-gassed at 200 °C for 2 h prior to the measurement. The surface area was calculated using the BET (Brunauer–Emmett–Teller) method. The total volume (V_{tot}) was estimated as the liquid volume of N_2 at relative pressure of 0.98. The volume of micropores (V_{DR}) was determined by the Dubinin–Radushkevich (DR) method. The mesopore volume (V_{mes}) was calculated by subtracting V_{DR} from V_{tot} [25,26]. The C, H, N elemental composition was measured by an elemental analyzer (PE-2400 series. PerkinElmer Inc.). SEM analyses were carried out on a scanning electron microscope (SM-300, Hitachi Corp., Japan). The dried samples were coated with a thin gold film to give electrical conduction on the carbon external surface. Ca, K, Si and Fe contents were determined using an energy dispersive X-ray spectrometer (Rayny EDX-800, Shimadzu Corp., Japan). The powder X-ray diffraction (XRD) patterns of the samples were recorded on an X-ray diffractometer (RINT 2100, Rigaku Industrial Corp., Japan) with Cu-K_α irradiation (40 kV, 40 mA). The pH of the suspension of MFS-derived material was measured using a pH meter (Seveneasy S-20, Mettler Toledo Corp., Japan). 0.05 g dry adsorbent powder was added to 50 mL distilled water. The suspension was stirred overnight prior to the determination.

2.3. Copper adsorption

A Cu(II) stock solution was prepared by dissolving copper(II) sulfate in deionized water at 1000 mg L^{-1} of Cu(II). The stock solution was diluted with deionized water to the desired concentrations. Kinetic studies were conducted at 25 °C in a water bath shaker.

Table 1
Elemental compositions and surface properties of MFS and MFS-derived adsorbents.

Sample	Atmosphere	Temperature (°C)	Time (h)	Ash (%)	EDX					Elemental analysis			S_{BET} ($m^2\,g^{-1}$)	V_{tot} ($mL\,g^{-1}$)	V_{DR} ($mL\,g^{-1}$)	V_{mes} ($mL\,g^{-1}$)	V_{mes}/V_{tot} (%)	Dp (nm)
					Si, %	Ca, %	Fe, %	K, %	Mn, %	C, %	H, %	N, %						
MFS (dry basis)	–	–	–	30.9	13.2	9.0	4.6	2.1	0.13	35.38	4.81	3.60	–	–	–	–	–	–
CN500	N_2	500	1	58.1	26.6	18.5	8.9	2.2	0.29	29.03	1.33	2.27	150.7	0.1891	0.0812	0.1079	57.1	5.0
CN700	N_2	700	1	64.1	32.2	18.1	11.0	3.4	0.28	29.84	0.92	1.41	196.1	0.2248	0.0972	0.1276	56.8	4.6
CF21N7	N_2	700	1	71.1	34.4	12.4	26.8	1.2	0.23	26.16	1.04	1.48	244.6	0.2429	0.1198	0.1231	50.7	4.0
CS500	Steam	500	1	56.8	32.3	14.9	8.3	2.2	0.20	29.02	1.16	2.18	157.0	0.1966	0.0890	0.1076	54.7	5.0
CS700	Steam	700	1	71.5	37.6	19.7	10.9	3.7	0.27	19.92	0.43	0.80	212.3	0.2557	0.1025	0.1532	59.9	4.8
CF21S7	Steam	700	1	80.7	32.6	15.9	30.5	1.8	0.29	16.66	0.58	0.53	231.1	0.2487	0.1175	0.1312	52.8	4.3

50 mL aqueous solution with 100 mg L^{-1} Cu(II) was mixed with 0.05 g adsorbent in a conical flask and agitated at 100 rpm. The adsorbent was separated from the solution at different time intervals. The concentration of Cu(II) in the solution was analyzed by flame atomic absorption spectrometry (AAnalyst 200, PerkinElmer Inc.). For the equilibrium experiment, 0.05 g adsorbent was added to 50 mL Cu(II) solution of the desired initial concentrations in sealed conical flasks. The mixtures were agitated at 100 rpm in a water bath at 25 °C. The solutions were filtered at equilibrium and the concentrations of Cu(II) were determined by AAS method. The effect of pH on the removal of copper was also studied. The initial pH of copper solution with the concentration of 100 mg L^{-1} was adjusted to 2–6 (above 6 copper precipitation occurs) using 0.1 M HCl or 0.1 M NaOH solution. The adsorption capacity was estimated after reaching equilibrium.

2.4. Copper desorption

The irreversibility of copper adsorption onto MFS-derived material was investigated by carrying out desorption studies in batch process. 50 mL aqueous solution with 200 mg L^{-1} Cu(II) was contacted with 0.05 g adsorbent by shaking at 25 °C to reach equilibrium. The solution was then filtered and the filtrate was analyzed to determine the Cu(II) concentration. The copper saturated adsorbent was transferred to 50 mL deionized water in another conical flask at 25 °C with 100 rpm agitation for 24 h. The adsorbent was removed and the concentration of Cu(II) desorbed in the aqueous solution was determined by AAS method. The copper desorption in a 0.2 M HCl aqueous solution was also carried out for comparison [7].

3. Results and discussion

3.1. Characterization of the adsorbents

Some structural and chemical features of MFS-derived adsorbents are shown in Table 1. All MFS-derived materials possess intermediate BET surface area (150–250 $m^2 g^{-1}$) and developed mesoporosity (average pore diameter 4.0–5.0 nm). It has been reported that surface area of sludge-derived materials higher than 200 $m^2 g^{-1}$ cannot be directly achieved by pyrolysis or gasification [3]. CF21N7 and CF21S7 show a surface area higher than 200 $m^2 g^{-1}$ due to the introduction of $Fe(NO_3)_3$. The scanning electron microscopy (SEM) technique was also employed to observe the surface morphology of MFS-derived adsorbents. The irregular shape solids containing pores with different sizes are observed. It was found that the increase of pyrolysis temperature can enhance the solid porosity.

The results of elemental analyses and EDX are also shown in Table 1. All MFS-derived adsorbents possess high content of inorganic matter (56–80%), which leads to a relatively strong surface basicity (pH 9.3–11.2). It is notable that iron contents in the MFS-derived materials were of 8.9 and 11.0% for CN500 and CN700; 8.3 and 10.9% for CS500 and CS700; whereas 27.2 and 37.8% for CF21N7 and CF21S7 respectively. There are many different forms of iron (hydr)oxides, e.g., Fe_2O_3, FeOOH, Fe_3O_4 and Fe_2O_4, which can be determined by X-ray diffraction analysis. The XRD patterns in Fig. 1 are not able to determine the crystal structure of iron (hydr)oxides on the materials prepared at low pyrolysis temperature; revealing that the iron (hydr)oxides randomly distribute on the matrix of carbons and their clusters are too small to form clear X-ray diffraction patterns. No magnetite (Fe_3O_4) phase was founded in all MFS-derived materials. The iron (hydr)oxides in CN500, CN700, CS500 and CS700 were identified as a mixture of FeOOH, Fe_2O_3 and Fe_2O_4, whereas those in CF21N7 and CF21S7 were a mixture of predominant Fe_2O_4 and Fe_2O_3.

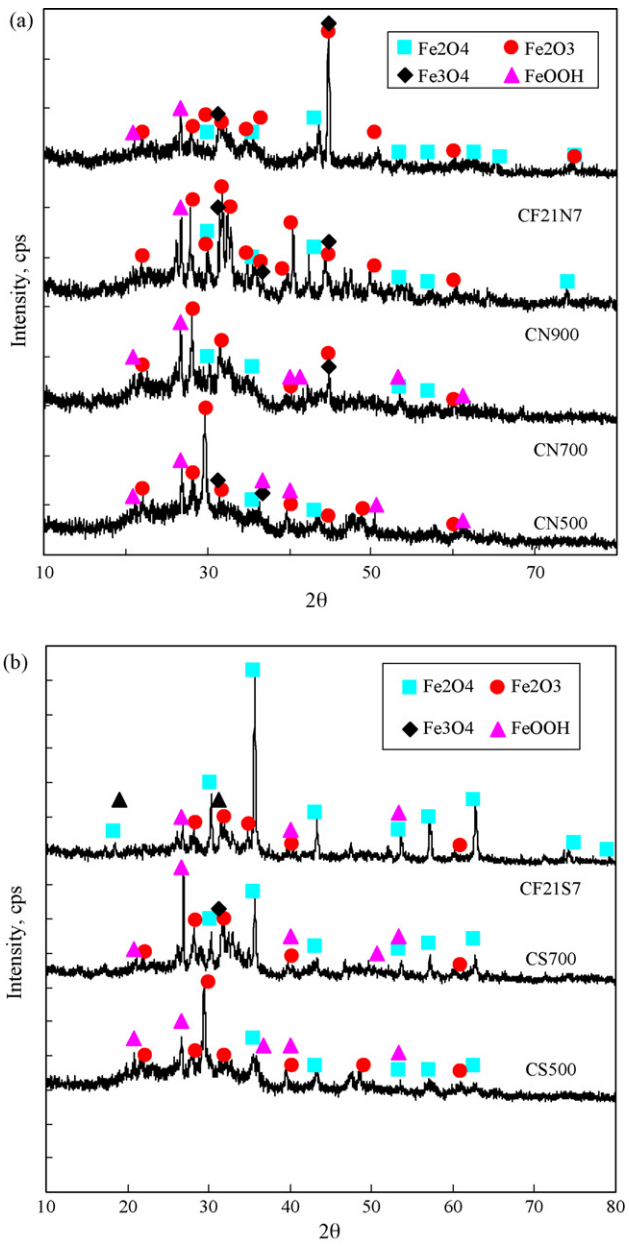

Fig. 1. XRD patterns of MFS-derived materials.

3.2. Effect of pH

Copper removal may be the result of complexation with previously adsorbed water molecules or may occur via a cation-exchange mechanism. As shown in Fig. 2a, the initial pH of Cu(II) aqueous solutions at various concentrations are in the range of 4.9–5.6 because of the hydrolysis of Cu^{2+} to various extents. They shift to basic range when the solutions contact with the MFS-derived materials. However, it is evidence that the equilibrium pH value of aqueous solution decreases with increasing initial Cu(II) concentration. In the case of Cu(II) aqueous solution with low initial concentration (<50 mg L^{-1}), the equilibrium pH is higher than 6.0, which could result from the surface precipitation reaction of copper ions. However, for the solution with relatively high initial concentration (>100 mg L^{-1}), the equilibrium pH is lower than 6.0,

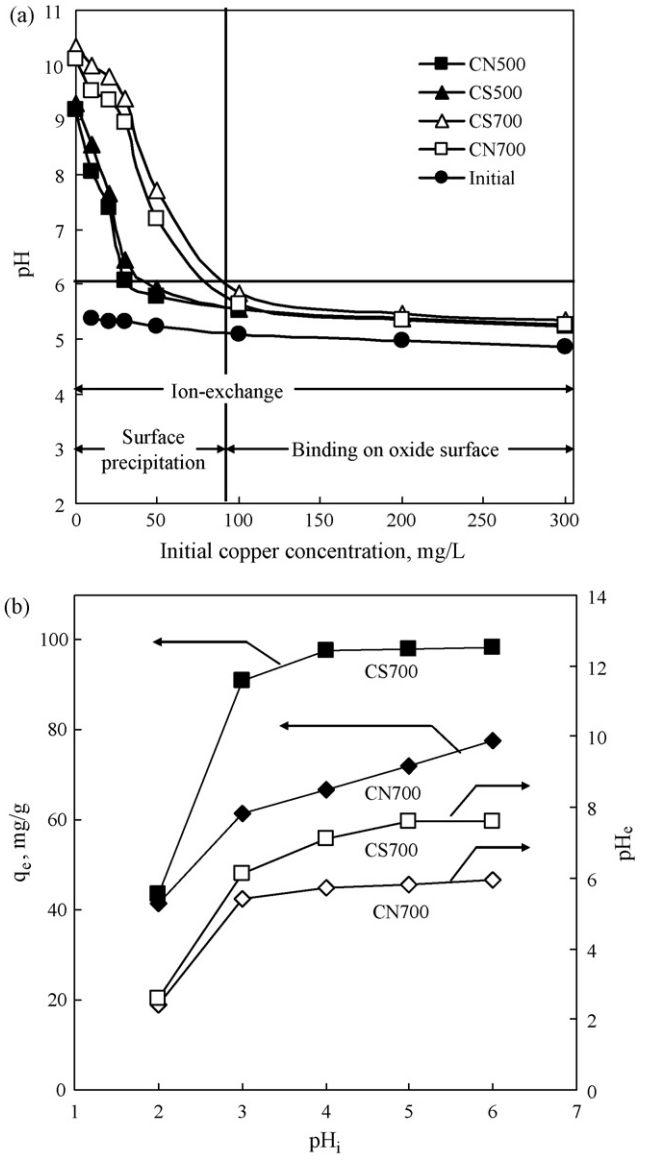

Fig. 2. (a) Change in pH value of aqueous solution by copper adsorption and (b) effect of adjusted initial pH value on copper adsorption.

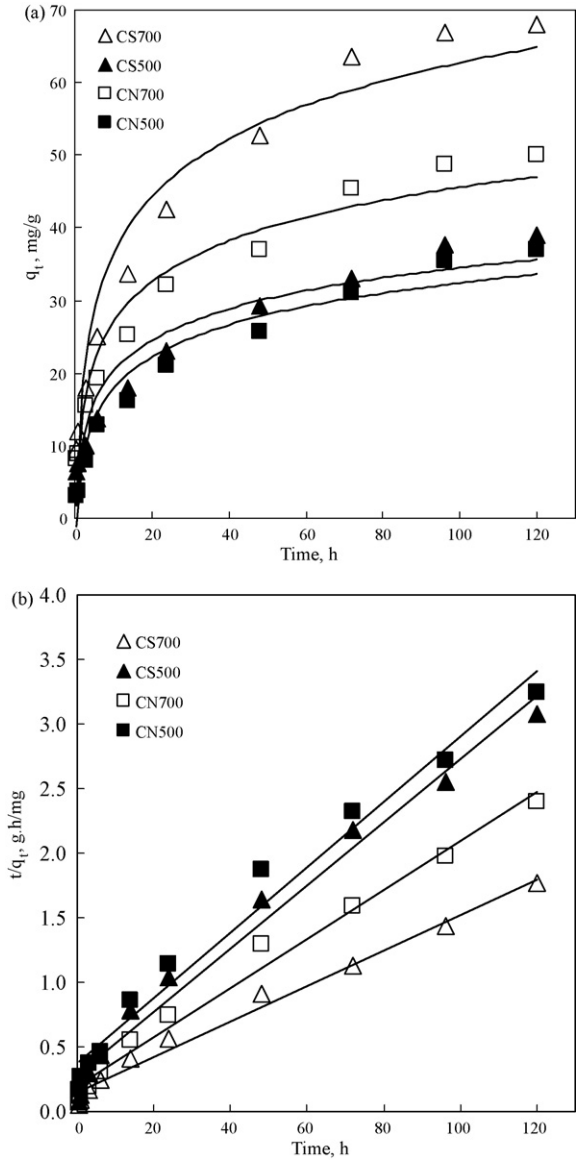

Fig. 3. Adsorption kinetics: (a) effect of contact time and (b) pseudo-second-order plots.

therefore, ion-exchange and binding on the iron (hydr)oxides surface are the predominant pathway for the removal of Cu(II) from the aqueous solution.

The effect of pH on the adsorption of copper onto the MFS-derived adsorbents was studied in the range $2 < pH < 6$. The result in Fig. 2b shows that a higher pH leads to a higher copper ion adsorption capability at the experimental conditions. Due to the increase of pH, more surface functional groups dissociate to provide metal binding sites, which results in a high metal ion adsorption. This can be related to a decrease in the competition between the proton (H^+) and the positively charged metal ion at the surface sites.

3.3. Adsorption kinetics

The effect of contact time on Cu(II) adsorption is shown in Fig. 3a. It is clear that adsorption is a rapid step at the beginning (2 h), followed by a much slower second step, possibly related to solid-state diffusion. The experimental data for Cu(II) adsorption kinetics were analyzed using the pseudo-first-order kinetics model (Eq. (1)) and the pseudo-second-order kinetics model (Eq. (2)) respectively.

$$\mathrm{Log}(q_e - q_t) = \log q_e - \frac{k_1 t}{2.303} \quad (1)$$

$$\frac{t}{q_t} = \frac{t}{q_e} + \frac{1}{k_2 q_e^2} \quad (2)$$

where q_e in mg g^{-1} is the maximum adsorption capacity, q_t in mg g^{-1} represents the amount of copper adsorbed at various times t, k_1 in min^{-1} is the rate constant of pseudo-first-order adsorption, while k_2 in g mg^{-1} min^{-1} is the rate constant of pseudo-second-order adsorption. The pseudo-first-order equation shows a poor correlation with the experimental data, whereas the pseudo-second-order equation indicates a good correlation of the experimental results with linearized form (in Fig. 3b). The fitting parameters are tabulated in Table 2. The data indicate that copper is adsorbed following the pseudo-second-order kinetic model with correlation coefficient $R^2 > 0.98$.

Table 2
Parameters for copper adsorption onto MFS-derived adsorbents.

Sample	Pseudo-second-order $\frac{t}{q_t} = \frac{t}{q_e} + \frac{1}{k^2 q_e^2}$			Langmuir $C_e/q_e = C_e/q_m + 1/(k_L q_m)$			Freundlich $q_e = k_F C_e^{1/n}$		
	k_2 (g mg^{-1} min^{-1})	q_e (mg g^{-1})	R^2	q_m (mg g^{-1})	k_L (L mg^{-1})	R^2	k_F	$1/n$	R^2
CS500	1.3×10^{-3}	72.46	0.9869	45.25	0.069	0.9917	15.03	0.193	0.9656
CS700	1.9×10^{-3}	52.36	0.9848	86.96	0.081	0.9904	27.27	0.206	0.9457
CN500	2.1×10^{-3}	40.82	0.9799	42.37	0.063	0.9924	20.05	0.111	0.9842
CN700	1.7×10^{-3}	39.53	0.9778	61.35	0.052	0.9884	24.59	0.149	0.9753

3.4. Adsorption isotherms

Although the true equilibrium cannot be attained in short-term experiment, pseudo-equilibrium conditions are attained at about 72 h for all samples. Accordingly, the experiments for effect of initial concentration were carried out for 96 h contact time. The curves in Fig. 4a exhibit L-shape according to the Giles classification, suggesting the favorable adsorption of Cu(II) for all cases. The Langmuir (Eq. (3)) and Freundlich (Eq. (4)) adsorption isotherm models were applied to analyze the experimental data of equilibrium adsorptions.

$$\frac{C_e}{q_e} = \frac{C_e}{q_m} + \frac{1}{(k_L q_m)} \tag{3}$$

$$q_e = k_F C_e^{1/n} \tag{4}$$

where q_m in mg g^{-1} and k_L in L mg^{-1} are Langmuir constants related to sorption capacity and energy of sorption, whereas k_F and $1/n$ are the Freundlich constants related to the sorption capacity and intensity respectively. The Langmuir and Freundlich parameters correspond to the fitting of experimental results are shown in Table 2. The performance of MFS-derived materials for copper adsorption is comparable to that reported in a literature [27]. The highest capacity with a value of 87 mg g^{-1} was found for CS700. The Langmuir plots give a linear form (in Fig. 4b) and show a better fit to experimental data than the Freundlich model. This suggests that, in spite of chemical complexity of the MFS-derived adsorbents, their adsorption sites can be considered to be in proportion to copper adsorption capability. This must be related to the mechanism of adsorption, which is via cation-exchange or surface precipitation reaction. The affinity between Cu(II) and MFS-derived adsorbent can be predicted by dimensionless constant separation factor R_L, which is defined by the following equation (Eq.(5)), according to Hall et al. [28]:

$$R_L = \frac{1}{(1 + k_L C_0)} \tag{5}$$

where C_0 in mg L^{-1} is the initial Cu(II) concentration. The adsorption process as a function of R_L may be described as: $R_L > 1$, unfavorable; $R_L = 1$, linear; $0 < R_L < 1$, favorable; and $R_L = 0$, irreversible. The Plots of R_L versus initial Cu(II) concentration for respective adsorbents are shown in Fig. 5. The values are found to be of 0.03–0.35, indicating that the adsorption of Cu(II) on the MFS-derived adsorbent is favorable. Moreover, at high initial Cu(II) concentrations, the values of R_L are less than 0.1, suggesting the occurrence of irreversible adsorption.

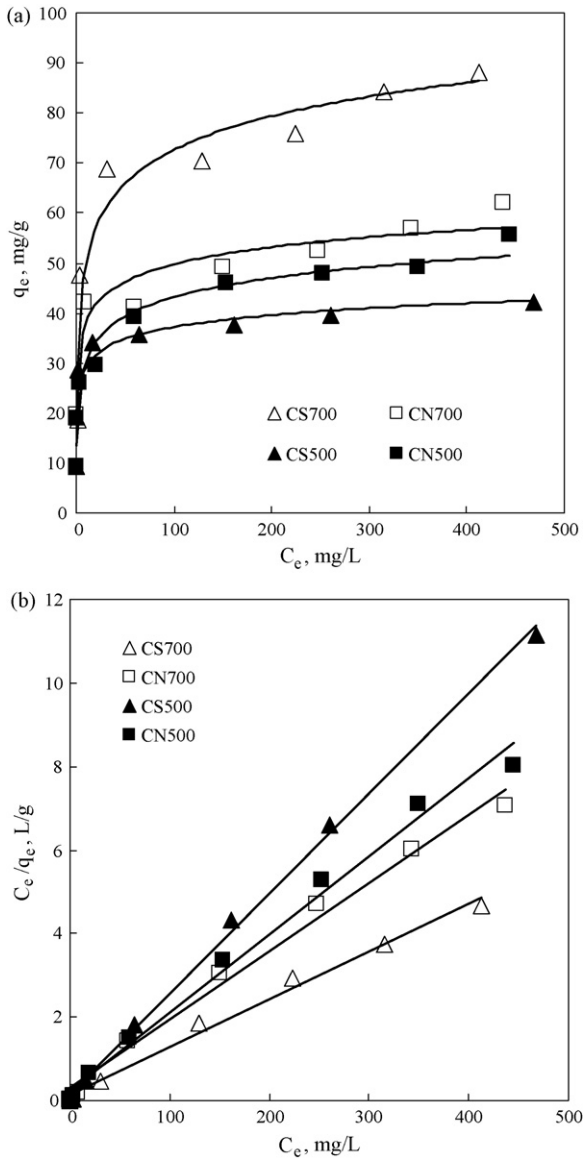

Fig. 4. Adsorption isotherms: (a) effect of initial Cu(II) concentration (b) Langmuir plots.

3.5. Effect of iron oxide content and forms

The effect of iron content on removal of Cu(II) is presented in Fig. 6. The adsorption rises to a maximum value with increase the iron content form 8.3 to 11.2%. Although CF21N7 and CF21S7 possess much higher iron contents than CN700 and CS700, the Cu(II) adsorption capacity of the former two samples shows much lower than that of the latter two. The result shows that the iron (hydr)oxides in MFS-derived adsorbents may affect the removal of copper not only through their content but also through their forms in the surface. Iron (hydr)oxides in CF21N7 and CF21S7 have been identified as a mixture of Fe_2O_4 and Fe_2O_3 by XRD, whereas those in CN700 and CS700 are a mixture of FeOOH, Fe_2O_4 and Fe_2O_3. It has been reported that FeOOH possesses high removal capability for some heavy metals [16–18]. Moreover, Hu et al. [22] has given the evidence that δ-FeOOH shows higher capability to remove Cr(VI) from synthetic wastewater than γ-Fe_2O_3.

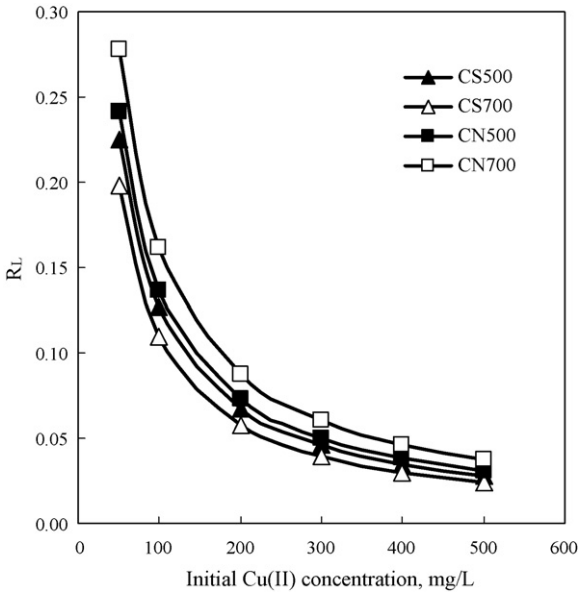

Fig. 5. Plots of R_L versus initial Cu(II) concentration.

3.6. Change in adsorbents composition

The EDX spectra for copper-loaded CN700 are shown in Fig. 7, and the changes in amount of iron, calcium, potassium and copper as a function of initial Cu(II) concentration are presented in Fig. 8. Peaks for Cu-K_α and Cu-K_β are observed in Fig. 7 after exposure to copper aqueous solution, and their intensity increases with increasing initial Cu(II) concentration, revealing the occurrence of Cu(II) adsorbs onto the surface of CN700 and the adsorption increases with progression of initial Cu(II) concentration. It is interesting that raising the initial Cu(II) concentration can lead to decrease the intensity of Ca-K_α and Ca-K_β but almost cause no change in the intensity of Fe-K_α and Fe-K_β. This suggests that the removal of Cu(II) occurs based on cation-exhange with Ca^{2+}, K^+ and H^+ rather than with iron cation.

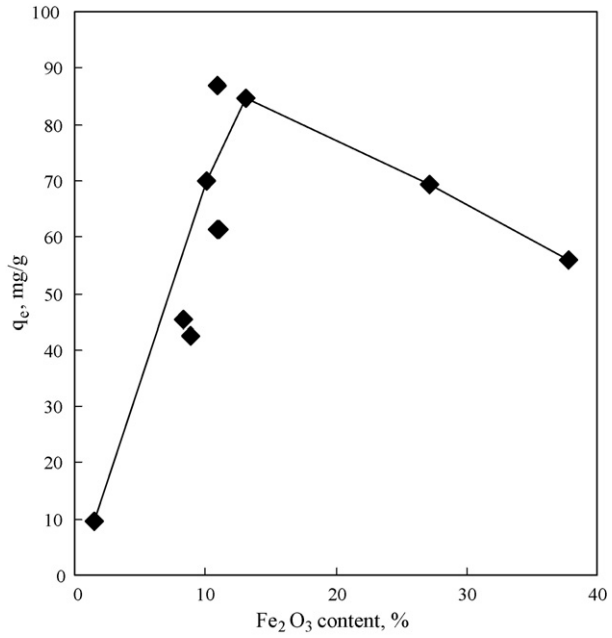

Fig. 6. Effect of iron content on copper adsorption.

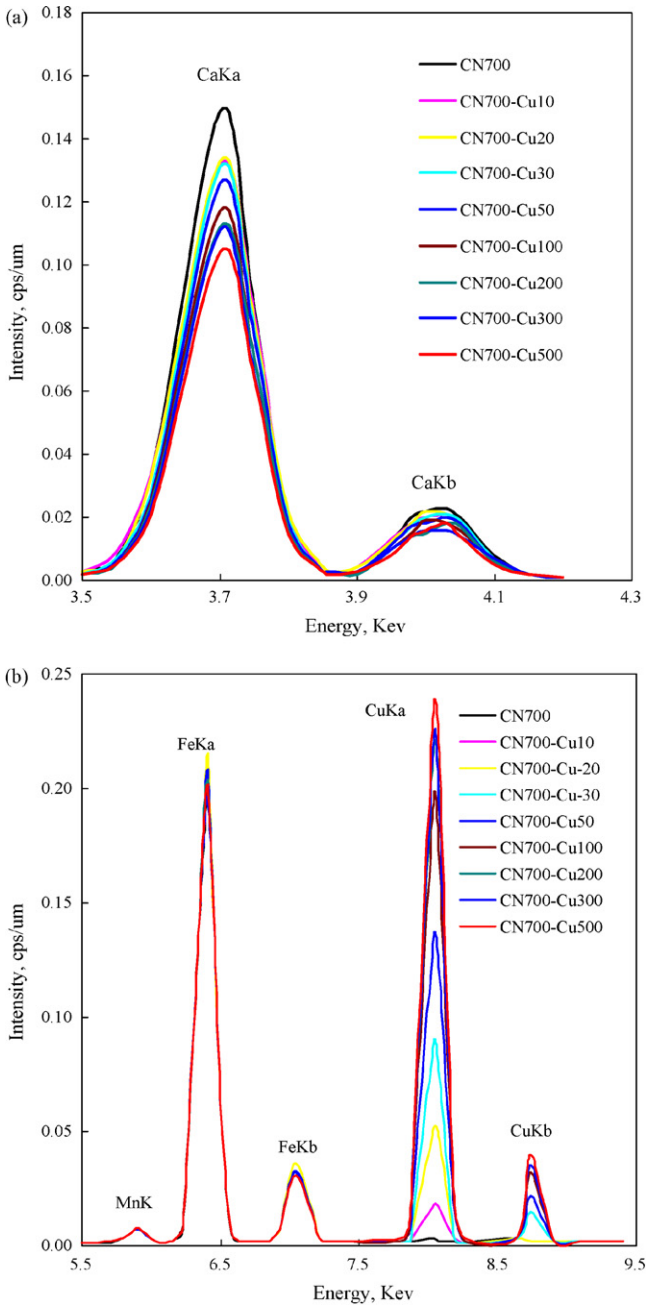

Fig. 7. Spectra of EDX for MFS-derived materials after exposure to copper aqueous solutions with various initial concentrations.

3.7. Desorption studies

Desorption of Cu(II) from the MFS-derived adsorbents was examined so as to understand the adsorption mechanism and evaluate the immobilization of copper species in the adsorbents. The results showed that the desorption of copper from MFS-derived materials was quite low, and less than 1% of the adsorbed copper was recovered. This could suggest that strong bonds are created between the surface of MFS-derived materials and copper ion, and the irreversible reactions occur during the process of adsorption, therefore, the adsorbent can be applied to the immobilization of copper in water or soil. However, about 35–42% of loaded Cu(II) desorbed in 0.2 M HCl solution. It is evidence that Cu(II) adsorbed via surface precipitation can be recovered by acid solution.

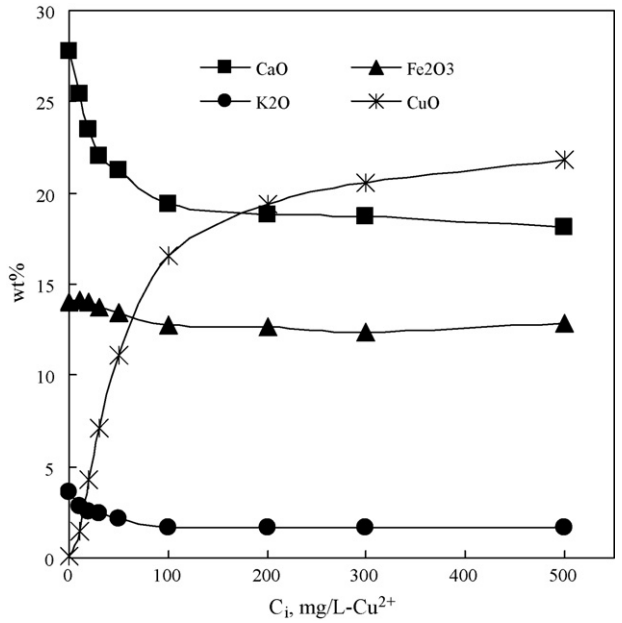

Fig. 8. Change in amounts of various metals.

3.8. Mechanism of copper adsorption

It is likely that the oxides in the MFS-derived materials are positively charged from pH 4 to 6 by the adsorption of H^+, while they become negatively charged from pH 6 to 8 by the adsorption of OH^-. Therefore, the amphoteric adsorption sites may exist in one of three protonation states: weak acidic sites ≡S–OH_2^+ between pH 4 and 6; weak basic sites ≡S–OH in the range of pH 6–8 and basic sites ≡S–O^- at pH > 8 [28]. In which ≡S represents the surface of MFS-derived adsorbents. It is previously proposed that the adsorption Cu(II) onto MFS-derived materials is based on ion-exchange with Ca^{2+}, K^+ and H^+ and/or precipitation on surfaces and/or binding with active sites on the surface of amorphous ion oxides and/or hydroxides. The adsorption behavior is strongly affected by pH value because that Cu(II) can form various species such as $[Cu_2(OH)_2]^{2+}$, $[Cu(OH)]^+$, $Cu(OH)_2$, $[Cu(OH)_3]^-$ and $[Cu(OH)_4]^{2-}$ by hydrolysis of Cu^{2+} in aqueous solutions at various pH values. Accordingly, the mechanism of Cu(II) adsorption onto the surfaces of MFS-derived materials can be expressed as follows:

(1) At 4 < pH < 6, Cu^{2+} is the dominant copper ion in aqueous solution, whereas ≡S–OH_2^+ and ≡S–OH are present on the surface of adsorbents. Accordingly, the adsorption of Cu(II) will occur via ion-exchange with protons or binding on the surfaces of iron oxides and/or hydroxides.

(i) Ion-exchange with protons

$$2{\equiv}S\text{–}O\text{–}H_2^+ + Cu^{2+} \rightarrow ({\equiv}S\text{–}O)_2\text{–}Cu + 4H^+ \quad (6)$$

$$2{\equiv}S\text{–}O\text{–}H + Cu^{2+} \rightarrow ({\equiv}S\text{–}O)_2\text{–}Cu + 2H^+ \quad (7)$$

(ii) Binding on the surface of iron oxides and/or hydroxides

≡FeOH and ≡FeOOH represent the active sites on the surface of iron hydrous oxides, which exists on the surface of MFS-derived materials. Therefore, the adsorption of Cu(II) can be described as postulating bidentate bonding reaction ((8) and (9)) or simultaneous adsorption and hydroxylsis reaction ((10) and (11)):

$$2{\equiv}FeOOH + Cu^{2+} \rightarrow ({\equiv}FeO)_2Cu + 2H^+ \quad (8)$$

$$2{\equiv}FeOH + Cu^{2+} \rightarrow ({\equiv}FeO)_2Cu + 2H^+ \quad (9)$$

$${\equiv}FeOOH + Cu^{2+} + H_2O \rightarrow {\equiv}FeOOCuOH + 2H^+ \quad (10)$$

$${\equiv}FeOH + Cu^{2+} + H_2O \rightarrow {\equiv}FeOCuOH + 2H^+ \quad (11)$$

(2) At pH range of 6–8, Cu^{2+}, $[Cu_2(OH)_2]^{2+}$ and $[Cu(OH)]^+$ become the main copper ions in aqueous solution and ≡S–O^- is the dominant active sites on the surface of MFS-derived adsorbents. As a result, Cu(II) will be removed through ion-exchange with Ca and K ions, and precipitation either as a surface precipitation or as a bulk precipitation.

(i) Ion-exchange with Ca^{2+} or K^+

$$({\equiv}S\text{–}O)_2\text{–}Ca + Cu^{2+} \rightarrow ({\equiv}S\text{–}O)_2\text{–}Cu + Ca^{2+} \quad (12)$$

$$({\equiv}S\text{–}O)_2\text{–}Ca + 2CuOH^+ \rightarrow 2{\equiv}S\text{–}O\text{–}CuOH + Ca^{2+} \quad (13)$$

$$2{\equiv}S\text{–}O\text{–}K + Cu^{2+} \rightarrow ({\equiv}S\text{–}O)_2{\equiv}Cu + 2K^+ \quad (14)$$

$${\equiv}S\text{–}O\text{–}K + CuOH^+ \rightarrow {\equiv}S\text{–}O\text{–}CuOH + K^+ \quad (15)$$

(ii) Binding on surface of iron hydroxide and/or oxide

$${\equiv}FeOOH + CuOH^+ + OH^- \rightarrow {\equiv}FeOOCuOH + H_2O \quad (16)$$

$${\equiv}Fe\text{–}OH + CuOH^+ + OH^- \rightarrow {\equiv}Fe\text{–}OCuOH + H_2O \quad (17)$$

(iii) Surface precipitation:

$${\equiv}S\text{–}O\text{–}H + 2Cu^{2+} + 4OH^- \rightarrow {\equiv}S\text{–}OCu_2(OH)_3(sp) + H_2O \quad (18)$$

(3) At pH > 9, besides surface precipitation, bulk precipitation occurs dominantly, and $Cu(OH)_2$ becomes the main copper species.

$$Cu^{2+} + 2OH^- \rightarrow Cu(OH)_2(s) \quad (19)$$

4. Conclusions

The conversion of sludge to carbon material by pyrolysis not only eliminates the need for further treatment of waste, but also produces a valuable adsorbent for water treatment. The results in this paper indicate the applicability of MFS-derived materials as adsorbent for the removal of Cu(II) from aqueous solution. CS700, the adsorbent obtained in a steam atmosphere at 700 °C for 1 h, shows the highest adsorption capacity of 87 mg g^{-1}, which is much higher than those of commercial activated carbons (between 8 and 50 mg g^{-1}). The high Cu(II) removal capacity of MFS-derived materials dues to their high iron (hydr)oxides content (8.3–11.0 wt%), strong surface basicity (pH 9.3–11.2) and intermediate surface area (150–200 m^2 g^{-1}). Besides, the form of iron (hydr)oxides also can affect the capability of copper adsorption. The Cu(II) removal process by MFS-derived materials is a strong pH-dependent, and can be dominantly classified as ion-exchange, surface precipitation and binding on the iron (hydr)oxides surface. The result of desorption experiment reveals that strong bonds are created between the oxide surface and Cu(II) due to the formation of inner-sphere metal surface complexes and metal hydroxide precipitate phases. The process of Cu(II) adsorption on MFS-derived adsorbent is irreversible, therefore, the adsorbent can be applied for removal of copper from aqueous solution or soil by fixation on the surface.

Acknowledgements

The research was financially supported by Agriculture, Forestry and Fisheries Research Council, Japan (Bio-recycle Project BUM-Cm3210, AFFRC). Support and service from National Institute for Rural Engineering (NIRE) is appreciated. The authors are grateful to Dr. Kunio Abe and Dr. Hideki Aihara, Wago Corp., Japan, for providing the sample of methane fermentation sludge.

References

[1] A. Bagreev, T.J. Bandosz, D.C. Locke, Pore structure and surface chemistry of adsorbents obtained by pyrolysis of sewage sludge-derived fertilizer, Carbon 39 (2001) 971–1979.

[2] A. Ros, M.A. Lillo-Rodenas, E. Fuente, M.A. Montes-Moran, M.J. Martin, A. Linares-Solano, High surface area materials prepared from sewage sludge-based precursors, Chemosphere 65 (2006) 132–140.

[3] M.A. Lillo-Rodenas, A. Rosb, E. Fuente, M.A. Montes-Moran, M.J. Martin, A. inares-Solano, Further insights into the activation process of sewage sludge-based precursors by alkaline hydroxides, Chem. Eng. J. 142 (2008) 168–174.

[4] M.J. Martin, A. Artola, M.D. Balaguer, M. Rigola, Activated carbons developed from surplus sewage sludge for the removal of dyes from dilute aqueous solutions, Chem. Eng. J. 94 (2003) 231–239.

[5] X. Wang, N. Zhu, B. Yin, Preparation of sludge-based activated carbon and its application in dye wastewater treatment, J. Hazard. Mater. 153 (2008) 22–27.

[6] C. Jindarom, V. Meeyoo, B. Kitiyanan, T. Rirksomboon, P. Rangsunvigit, Surface characterization and dye adsorptive capacities of char obtained from pyrolysis/gasification of sewage sludge, Chem. Eng. J. 133 (2007) 239–246.

[7] F. Rozada, M. Otero, A. Moran, A.I. Garcia, Adsorption of heavy metals onto sewage sludge-derived materials, Bioresour. Technol. 99 (2008) 6332–6338.

[8] F.S. Zhang, J.O. Nriagua, H. Itoh, Mercury removal from water using activated argons derived from organic sewage sludge, Water Res. 39 (2005) 389–395.

[9] M. Seredych, T.J. Bandosz, Sewage sludge as a single precursor for development of composite adsorbents/catalysts, Chem. Eng. J. 28 (2007) 59–67.

[10] J.H. Tay, X.G. Chen, S. Jeyaseelan, N. Graham, Carbon from digested sewage sludge and coconut hust, Chemosphere 44 (2001) 45–51.

[11] J.H. Tsai, H.M. Chiang, G.Y. Huang, H.L. Chiang, Adsorption characteristics of acetone, chloroform and acetonitrile on sludge-derived adsorbent, commercial granular activated carbon and activated carbon fibers, J. Hazard. Mater. 154 (2008) 1183–1191.

[12] L. Yu, Q. Zhong, Preparation of adsorbents made from sewage sludge for adsorption of organic materials from wastewater, J. Hazard. Mater. B137 (2006) 359–366.

[13] G.Q. Lu, D.D. Lau, Characterization of sewage sludge-derived adsorbents for H_2S removal, Gas Sep. Purif. 10 (1996) 103–111.

[14] W. Yuan, T.J. Bandosz, Removal of hydrogen sulfide from biogas on sludge-derived adsorbents, Fuel 86 (2007) 2736–2746.

[15] M.M. Rao, A. Ramesh, G.P.C. Rao, K. Seshaiah, Removal of copper and cadmium from the aqueous solutions by activated carbon derived from ceiba pentandra hulls, J. Hazard. Mater. B129 (2006) 123–129.

[16] M.M. Benjamin, Multiple-site adsorption of Cd, Cu, Zn and Pb on amorphous iron oxyhydroxide, J. Colloid Interf. Sci. 79 (1981) 209–221.

[17] A. Tessier, F. Rapin, R. Carignan, Trace metals in oxic lake sediments: possible adsorption onto iron oxyhydroxides, Geochim. Cosmochim. Acta 49 (1985) 183–194.

[18] D.C. Girvin, L.L. Ames, A.P. Schwab, J.E. McGarrah, Neptunium adsorption on synthetic amorphous iron oxyhydroxide, J. Colloid Interf. Sci. 141 (1991) 67–78.

[19] G.E. Millward, R.M. Moore, The adsorption of Cu, Mn, and Zn by iron oxyhydroxide in model estuarine solutions, Water Res. 16 (1982) 981–985.

[20] J.R. Bargar, G.E. Brown, G.A. Parks, Surface complexation of Pb (II) at oxide-water interfaces: II. XAFS and bond-valence determination of mononuclear Pb(I1) sorption products and surface functional groups on iron oxides, Geochim. Cosmochim. Acta 61 (1997) 2639–2652.

[21] H.J. Fan, P.R. Anderson, Copper and cadmium removal by Mn oxide-coated granular activated carbon, Sep. Purif. Technol. 45 (2005) 61–67.

[22] J. Hu, I.M.C. Lo, G. Chen, Performance and mechanism of chromate (VI) adsorption by δ-FOOH-coated maghemite (γ-Fe_2O_3) nanoparticles, Sep. Purif. Technol. 58 (2007) 76–82.

[23] S. Wu, A. Uddin, E. Sasaoka, Characteristics of the removal of mercury vapor in coal derived fuel gas over iron oxide sorbents, Fuel 85 (2006) 213–218.

[24] W. Chen, R. Parette, J. Zou, F.S. Cannon, B.A. Dempsey, Arsenic removal by iron-modified activated carbon, Water Res. 41 (2007) 1851–1858.

[25] Q. Qian, M. Machida, H. Tatsumoto, Preparation of activated carbons from cattle-manure compost by zinc chloride activation, Bioresour. Technol. 97 (2007) 353–360.

[26] Q. Qian, M. Machida, H. Tatsumoto, Textural and surface chemical characteristics of activated carbons prepared from cattle manure compost, Waste Manage. 28 (2008) 1064–1071.

[27] M. Seredych, T.J. Bandosz, Removal of copper on composite sewage sludge/industrial sludge-based adsorbents: the role of surface chemistry, J. Colloid Interf. Sci. 302 (2006) 379–388.

[28] K.R. Hall, L.C. Eagleton, A. Acrivos, T. Vermeulen, Pore and solid diffusion kinetics in fixed-bed adsorption under constant pattern conditions, Ind. Eng. Chem. Fundam. 5 (1966) 212–223.